Atmos. Meas. Tech. Discuss.,
doi:10.5194/amt-2016-292-AC1, 2016

Atmospheric Measurement Techniques Discussions

Interactive comment on "High resolution observations of small scale gravity waves and turbulence features in the OH airglow layer" *by* René Sedlak et al.

René Sedlak et al.

rene.sedlak@dlr.de

Received and published: 4 November 2016

The authors thank anonymous Referee #1 for the valuable and helpful comments.

The referee suggested that "the paper could connect better with previous work on 'ripples' [Hecht] and turbulence [Yamada] and stress what's new here." As was correctly noted by the referee the new instrument features higher spatial but also temporal resolution. We emphasized this by adding the following paragraph:

"Compared to earlier airglow imagers (Hecht et al., 1997, Yamada et al., 2001) the resolution has been improved by at least one order of magnitude in both space and time. Achieving a spatial resolution of 30 m/pixel (zenith angle of 46 °) and 17 m/pixel (zenith

Printer-friendly version

Discussion paper

angle of 0 °) the entire inertial subrange as well as the beginning viscous subrange of turbulence at airglow altitude is accessible to this instrument. Additionally, the temporal resolution of no longer than 2.8 s allows investigating the development of transient processes like breaking wave fronts." (lines 79-84)

Unfortunately, Y2001 don't give exact numbers for their horizontal resolution in units of meters, but judging from their overall field of view (FOV, 92°) and their detector size 1024 pixels, it may be estimated to be: 92°FOV/1024 pixels $\approx$ 0.09°/pixel => 87km*tan(0.09) $\approx$ 150m. H1997 smooth their initial resolution of 100km/516pixels in order to improve their signal-to-noise ratio, resulting in a resolution of approximately 750m/pixel. The temporal resolution of both Y2001 and H1997 is around one minute.

Due to these improvements the new instrument FAIM 3 can reveal features on scales significantly below one kilometre. In order to highlight these features we present two observations, the first one showing two periodic structures - and we agree with the referee, that even the larger one depicts an instability feature according to common opinion. As suggested by the referee we now refer to previous work of Hecht and Yamada on ripples and turbulence with the following new paragraph:

"While dynamical instability manifests as subordinate wave structures parallel to the initial wave fronts, convective instability emerges as wave structures perpendicular to the initial gravity wave (Andreassen et al., 1994; Fritts et al., 1994). Taylor and Hapgood, 1990 assume ripples to be the signature of KHIs, thus being related to dynamical instability. However, past observations do not agree about this issue. While Yamada et al., 2001 have presented images of instability features aligned parallel to a breaking gravity wave, Hecht et al., 1997 have observed ripple structures that were aligned perpendicular to an initial wave, which rather assigns those ripples to be caused by convective instability. In our observations none of both cases is favoured as the wave fronts of the 550 m wave packet are aligned by an angle of 45 ° to the superordinate 1.7 km wave. This supports the assumption of Hecht, 2004, that some ripples may be generated by the combination of dynamical and convective instability. According to

Fritts et al., 1996 an initially convectively driven instability structure can be rotated by the background wind shear." (lines 221-232)

In the second case study we present the turbulent breakdown of a wave front. FAIM 3 provides detailed observations of this transient event thanks to the high spatio-temporal resolution. In section 5 (discussion and summary) we added the following paragraph: "FAIM 3 not only resolves the entire inertial subrange, it also provides insight into the beginning viscous subrange of turbulence. As concerns airglow imaging this opens a new scale range of dynamic processes that can be monitored, like it is shown in the first case study. Whereas structures like the larger one (periodicity $\sim$ 1.7 km) can now be studied in greater detail with FAIM 3, structures like the smaller one (550 m) are now observable for the first time at all.

Concerning the connection of our observations with previous work in terms of scientific aspects, the second event is more evident. It shows the formation and temporal evolution of an instability feature. Due to the high temporal resolution (2.8 s) one can determine the initial formation of this structure and its later orientation relative to the initial wave field. Thus, observations of this kind are valuable for determining the nature of instability concerning the question whether such features are primarily driven convectively or dynamically.

In this context several former studies (e.g., Yamada et al., 2001, Hecht et al., 2004, Fritts et al., 1996) question whether "ripples" were initially formed parallel or perpendicular to the gravity wave fronts and then rotated by the local wind fields or formed as a combination of both instabilities. These possibilities severely complicate scientific interpretation of ripple occurrence. With the new observation capabilities provided by the FAIM 3 we can now study this initial formation in greater detail. The two instability events presented in this paper appear to be driven dynamically but in both cases there are also indications for the presence of convective instability, which suggests that these two instability mechanisms could actually accompany each other." (lines 290-305)

Of course, we are well aware of the fact, that complementary observations of the local wind field, temperature gradients etc. as provided by radars and/ or lidars are needed for a more sophisticated investigation of these cases. But the intention of our study is to give a proof of concept concerning the capabilities of highly resolved airglow observations. Furthermore the referee commented that discussing the observations with numerical modelling, “more specific discussions are needed”. Since the overall aim here is to show the ability of our new imager to observe small-scale wave structures and turbulence features on scales significantly below 1 km, we decided to just give a rough qualitative comparison to numerical modelling. Closer investigations concerning the numerical simulations are beyond the scope of this paper and will be treated in future studies. In lines 308 ff. we added the paragraph

"The typical vortex structures and the decay into eddies also appear in the respective airglow modelling. Like outlined there and in the companion experimental paper (Hecht et al., 2014), the simulations have predicted such small features that could not have been resolved by airglow imagers at that time.“ Referring to the minor comments:

1. We added “(shortwave infrared, commonly defined from 0.9 to 1.7 μm)” behind “SWIR” in line 29 f. 2. We dropped ‘frequently’ in line 39. 3. Changed as suggested. New Version: “Energy and momentum transported . . . are . . .” in line 45. 4. Line 57-59: Removed as suggested. 5. We indeed mean 299 km2 as this is the horizontal area of the trapezium-shaped FOV of FAIM 3 under a zenith angle of 46 $^{\circ}$. The parallel sides of the trapezium are 15.2 km and 16.9 km and the height of the trapezium is 18.6 km. (line 98) 6. Yes, the temporal evolution of the image series suggests that the wave packet is advected by the background wind. The respective sentence in the paper has been extended by “[the wave packet is] apparently advected by the background wind” (line 146 f.)

7. The order N of the MEM, meaning the length of the underlying AR model when using Burg’s algorithm, has been raised to a value of 36. As it has been outlined in section 3 and is described more detailed by (Wüst & Bittner, 2006), using the MEM, there is

a certain range of orders rather than the one correct order to best resolve a certain wavelength. The fact that the 550m peak stays stable after raising the order from 20 to 36 (still talking about the same data series with a length of 59) indicates that this wavelength has been fully resolved. We added "[The order] of the MEM" in line 166 f. to make it clearer.

8. Figure 6: The Referee remarked that the vortex and filaments mentioned in the text would be hard to recognize in Figure 6 and that some help would be needed. We expanded the number of images from six to fifteen. In order to better guide the reader's eye we outlined six dominating structures of this transient event and focused on describing their respective temporal evolution.

We have revised the description of the event according to the more detailed visualization in Figure 6 as follows:

"A wave front, indicated by the dashed black line in the images of Figure 6, enters the FOV in the upper right corner. While it continues propagating to the lower left, a filament separates from it on the left side (Figure 6a – b, orange). This filament moves much slower than the wave front. At around 03:18:30 UTC (Figure 6c) a second filament structure becomes visible below the first filament. In the further course of the image series (Figure 6e – f) it turns out to separate into two structures, a filament moving downward (yellow) and a stationary filament (green). At about 03:19:26 UTC (Figure 6g) the orange and the green structure begin to dissolve. The yellow structure continues propagating for a few more seconds and finally also starts decomposing at 03:19:54 UTC (Figure 6i). At 03:18:44 UTC (Figure 6d) two more filaments form at the upper right of the FOV right behind the initial wave front and are, in contrast to the other filaments, aligned perpendicular to it. They decompose at 03:19:26 UTC (Figure 6g). While the dynamics of the filaments take their course and form a vortex, rotating around a horizontally oriented axis, the initial wave front (black) overtakes the other structures, retaining its original direction (indicated by the red arrow in Figure 6h). At about 03:19:54 UTC (Figure 6i) another filament (blue) separates from it. This new

filament remains stationary and starts decaying at 03:20:50 UTC (Figure 6m). The wave front (black) keeps on propagating and leaves the FOV toward the lower left." (lines 173-185) and the caption of Figure 6 similarly.

9. Figure 7: We thank the referee for finding this mistake: the marked rectangle, which is meant to indicate the FOV of FAIM 3, is, with respect to the FAIM 4 all sky image, oriented in a wrong direction. Both cameras are adjusted in zenith position. The upper side of the FAIM 3 images corresponds to a direction of 303 ° and the upper side of the raw FAIM 4 images to a direction of 269 °. Additionally Figure 7 and Video 3 have been rotated northward and the red arrow, which indicates the direction of the propagating wave front in Figure 6, has been adopted to Figure 7. A north pointer has also been added to Figure 7, the western direction is also indicated. Instead of just marking the FAIM 3 FOV in the middle of the FAIM 4 image, we placed the respective FAIM 3 image in the revised Figure 7. Following the suggestion of Referee #2 we now also present a zoomed image (magnification factor 4).

We revised the text as follows:

"To put the observations into a larger spatial context, the FAIM 3 data are compared to simultaneous all sky measurements taken by the FAIM 4 instrument. Since the two cameras are deployed next to each other, the FOV of FAIM 3 is embedded in the centre of the FOV of FAIM 4. The FAIM 4 measurements are presented in Video 3. Besides the normal image the difference image (time difference of 60 s) is displayed on the right side; both images are rotated northward. The approximate FOV of FAIM 3 is indicated by the white boxes in Video 3. The all sky images reveal a clear and starry sky with high gravity wave activity, which can be determined on the basis of the characteristic patchy structures. The remarkable structure observed by FAIM 3 can be found again in Video 3 as a bright feature within the white box, propagating to eastern direction, which agrees with the FAIM 3 observations. Figure 7 shows the FAIM 4 all sky image at 03:20:20 UTC with the respective FAIM 3 image embedded into it (image a) as well as the image centre magnified by a factor of four (image b)." (lines 193-203) "The

aforementioned wave front is also visible in the all sky images, but a close inspection of Video 3 hardly allows perceiving indications for the separation of parts from the bright crest. Zooming into the all sky image (Figure 7b) shows that only the high-resolution measurements of FAIM 3 can reveal closer details of this structure." (lines 259-263)

"FAIM 4 all sky image taken on 5th April 2016 at 03:20:20 UTC (image a) and the magnified (zoom factor 4) image centre (image b). The entire sequence is shown in Video 3. Due to their spatial structure and their wavelength, we interpret the patchy structures in the starry sky as gravity wave fronts in the airglow layer. Comparison with the respective FAIM 3 image, which has been placed at its correct position in the middle of the all sky image shows how the small scale details of the wave crest can be resolved with the new instrument. The direction of propagation is indicated by the red arrow and matches with the observations of FAIM 3." (caption Figure 7)

Please also note the new version of Video 3, which has been submitted.

Please also note the supplement to this comment:
http://www.atmos-meas-tech-discuss.net/amt-2016-292/amt-2016-292-AC1-supplement.zip

---

Interactive comment on Atmos. Meas. Tech. Discuss., doi:10.5194/amt-2016-292, 2016.

Printer-friendly version

Discussion paper

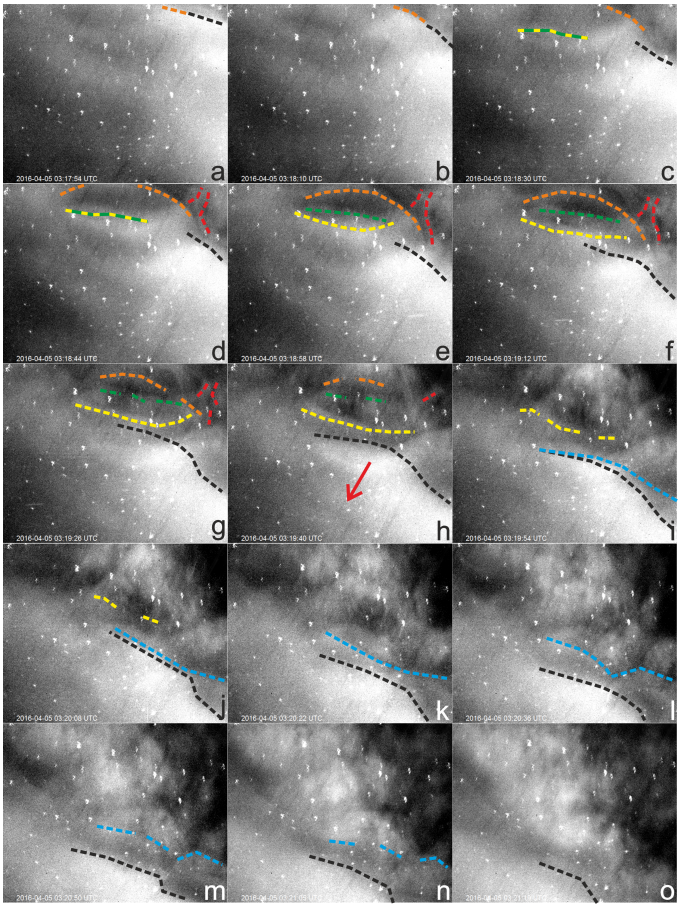

Fig. 1. Figure 6 revised

Printer-friendly version

Discussion paper

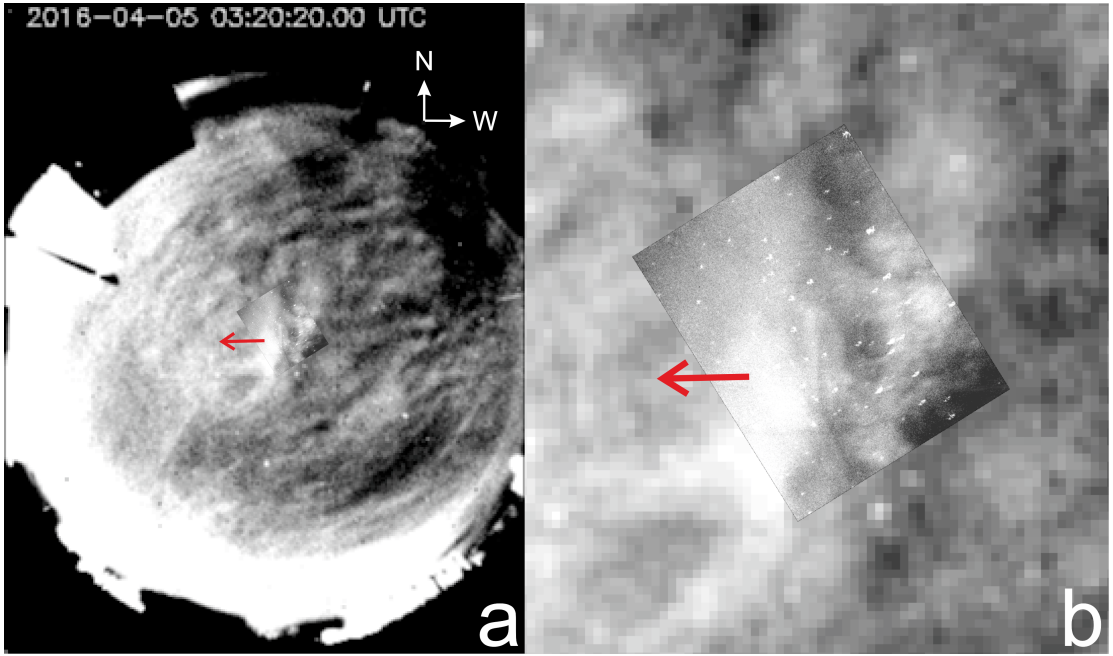

Fig. 2. Figure 7 revised

Printer-friendly version

Discussion paper